

Optimization of light illumination for photoacoustic computed tomography of human infant brain

Sadreddin Mahmoodkalayeh ^{a,c}, Xun Lu ^b, Mohammad Ali Ansari ^c, Hengguang Li ^b,
Mohammadreza Nasirivanaki ^{d,e,f}

^aDepartment of Physics, Shahid Beheshti University, Tehran, Iran; ^bDepartment of Mathematics, Wayne State University, Detroit, MI, USA; ^cLaser and Plasma Research Institute, Shahid Beheshti University, Tehran, Iran; ^dDepartment of Biomedical Engineering, Wayne State University, Detroit, MI, USA; ^eDepartment of Neurology, Wayne State University School of Medicine, Detroit, MI, USA; ^fBarbara Ann Karmanos Cancer Institute, Detroit, MI, USA

ABSTRACT

Photoacoustic imaging (PAI) is an imaging modality for obtaining absorption coefficient at every location inside the tissue based on the detected photoacoustic signals. PA image reconstruction aims to determine the initial PA pressure everywhere inside the tissue. The pressure is proportional to both absorption coefficient and light fluence. Provided that fluence is homogenous, the reconstructed image will be an accurate mapping of the absorption coefficient of the tissue. Here we presented a method for obtaining uniform fluence inside the region of interest. We created a large dataset of fluence maps for different source locations, diameters and numerical apertures with Monte Carlo simulations, then used this dataset to solve an optimization problem for finding the source configuration which results in the best fluence distribution.

Keywords: Photoacoustic imaging, uniform illumination, optimization, Monte Carlo simulations.

1. INTRODUCTION

Photoacoustic imaging (PAI) is an emerging imaging modality which shows great potential for preclinical research and clinical practice [1-4] including brain imaging in both small animals [5-8] and humans [9-11]. Photoacoustic imaging (PAI) uses short laser pulses to illuminate the tissue, then the absorbed light energy turns into acoustic waves. Reconstructed images from photoacoustic (PA) signals are interpreted as distribution of absorption inside the tissue which further can be used for obtaining concentrations of chromophores. Different methods have been used to improve the PA signals and reconstructed images [12-15]. The PA pressure is proportional to both absorption coefficient, $\mu_a(r)$ and light fluence distribution, $F(r)$, inside the tissue. Provided that $F(r)$ is homogenous or uniform, the reconstructed image will be an accurate representation of the absorption coefficient of the tissue at a particular region. The goal of this study is to devise a PA-imaging system for imaging the entire human infant brain in which the light fluence distribution is uniform or as close as possible to it inside the head or at least inside some desired regions.

This device consists of a hemispherical helmet which houses a large number of optical fibers and ultrasound detectors. Several parameters are considered for optimization problem namely, the position of the optical fibers, diameter and the numerical aperture (NA) of the fibers. Using Monte Carlo simulation we create a large dataset of fluence maps for optical fiber for different diameters and numerical apertures. Then this dataset is used to

solve an optimization problem to find the configuration which produce a fluence as close as possible to a uniform distribution.

2. MATERIALS AND METHODS

2.1 Simulations and dataset generation

We used an infant head atlas model [16] which was segmented into six different regions, namely, extra cranial tissue (ECT) which is the combination of scalp and skull, cerebro-spinal fluid (CSF), gray matter, white matter, brain stem and cerebellum. We combined the cerebellum with gray matter and brain stem with white matter resulting in four different tissue types (Fig. 1). Voxels have a volume of 0.86 mm^3 . Optical properties tissues were selected similar to that of 800 nm light [17].

Then we devised an equidistant configuration on a hemisphere with 260 optical fibers and 120 ultrasound transducers (Fig. 2(a)). This hemisphere can be considered as a helmet which can be put on the infant's head as illustrated in Fig. 2(b). The gap between the helmet and head will be filled with ultrasound gel or water for impedance matching. We used water in the simulations. Locations of optical fibers are shown as red dots in Fig. 2(b) and each source has its own ID (srcID). To create our dataset we changed the diameter of the optical fibers and numerical apertures of the fibers. We considered ten different diameters from 0.5 to 5 mm in 0.5 mm steps and 5 different numerical apertures with $\text{NA}=0.11, 0.22, 0.3, 0.39$ and 0.5. These values are selected since they are available in practice. Then, Monte Carlo simulations are performed to obtain the fluence maps for each set of parameters and all 260 sources, amounting to a total simulation number of 13,000. For each run 100 million photons are simulated on GPU using MCX software [18]. After all simulation were completed we had a large dataset for each source and different parameters. Total fluence then could be calculated by adding the specified source to the current fluence map or subtracting it from the current from fluence map. It is as if we are turning on or off a specific source with specified parameters, namely the diameter and NA.

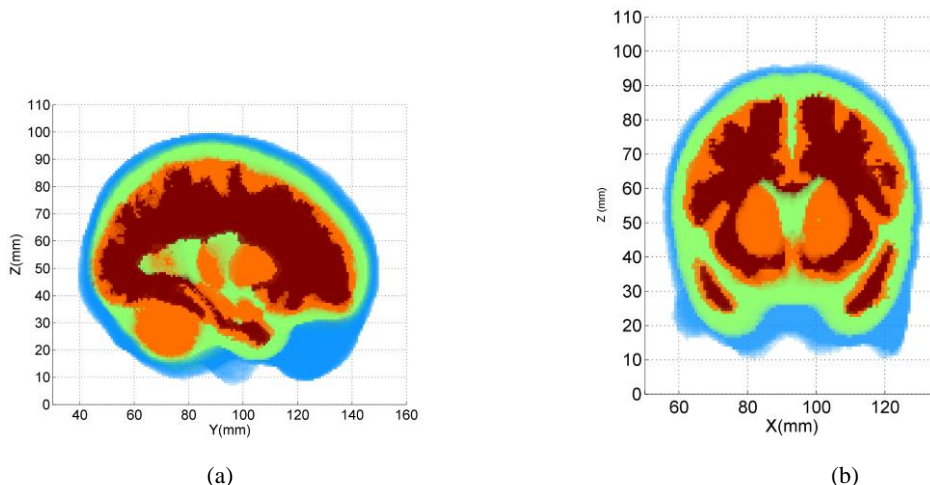


Figure 1. Infant head model used for simulations. Different colors represent different tissue types (blue: ECT, green: CSF, orange: gray matter and brown: white matter). (a) para-sagittal and (b) para-coronal cross-sections.

2.2 Optimization problem

Suppose we have N light sources, the positions of these light sources are fixed and the diameters are the same. We want to decide the diameter and the srcIDs to be turned on to obtain a uniform distribute fluence. We try to formulate this problem as an optimization problem

$$\min_{x \in X} \|F(x) - F_0\|_{L^2} \quad (1)$$

where x is a $N+1$ vector, the first N entries are binary variable, with 1 and 0 to indicate the corresponding srcID should be turned on and turned off, the last entry is the diameter to be chosen. To set up the problem we should specify the desired fluence map F_0 , the fluence map function $F(x)$, the cost function $\|F(x) - F_0\|_{L^2}$ and the constrains of variable x .

The Genetic Algorithm (GA) is a classic algorithm, which is a bio-inspired and population based technology for complex problems [19-21]. The algorithms are applicable to a wide range of optimization problems. This flexibility makes them attractive for many optimization problem in practice. GAs iteratively update a population of individuals. On each iteration, the individuals are evaluated using a fitness function. A new generation of the population is obtained by probabilistically selecting fitter individuals from the current generation. Some of these individuals are admitted to the next generation unchanged. Others are subject to genetic operators such as crossover and mutation to create new offspring. Here is a sketch of a typical GA in pseudocode in Fig. 3.

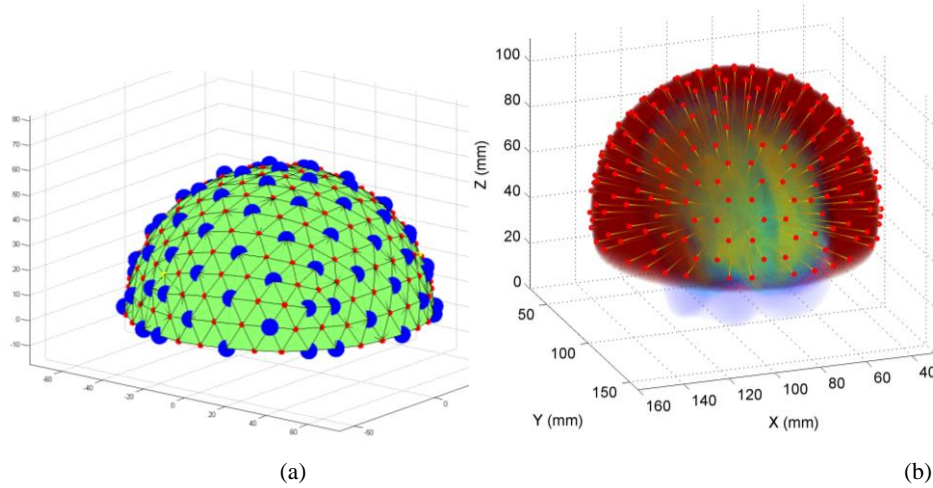


Figure 2. Helmet configuration design. (a) The configuration of optical fibers (red dots) and ultrasound transducers (blue circles), (b) placement of the helmet on the head with optical fibers sitting on the helmet.

Algorithm: GA(n, χ, μ)

```

1: % Initialize generation 0:
2:  $k := 0$ ;
3:  $P_k$ : = a population of  $n$  randomly generated individuals;
4: Evaluate  $P_k$ :
5: Compute fitness( $i$ ) for each  $i \in P_k$ ;
6: for  $i = 1$  to  $\delta$  do
7:   % Create generation  $k + 1$ :
8:   % 1. Copy:
9:   Select  $(1 - \chi) \times n$  members of  $P_k$  and insert into  $P_{k+1}$ ;
10:  % 2. Crossover:
11:  Select  $\chi \times n$  members of  $P_k$ ; pair them up; produce offspring; insert the offspring into  $P_{k+1}$ ;
12:  % 3. Mutate:
13:  Select  $\mu \times n$  member of  $P_{k+1}$ ; invert a randomly-selected bit in each;
14:  Evaluate  $P_{k+1}$ : Compute fitness( $i$ ) for each  $i \in P_{k+1}$ ;
15:  % Increment:
16:   $k := k + 1$ ;
17: end for
18: while fitness of fittest individual in  $P_k$  is not high enough;
19: return the fittest individual from  $P_k$ ;

```

Figure 3. Genetic Algorithm (GA)

3. RESULTS

3.1 Fluence maps

As said before, we can have resulting total fluence for each source configuration from our dataset. These fluence maps are used in the optimization problem when we are searching for the best configuration which gives us the fluence closest to the desired fluence f_0 . Fig. 4 shows resulted fluence maps for two different source configurations. We can select our regions of interest so we have the fluence map only for those regions. Fig. 4 shows the fluence map in only the gray and white matter tissues.

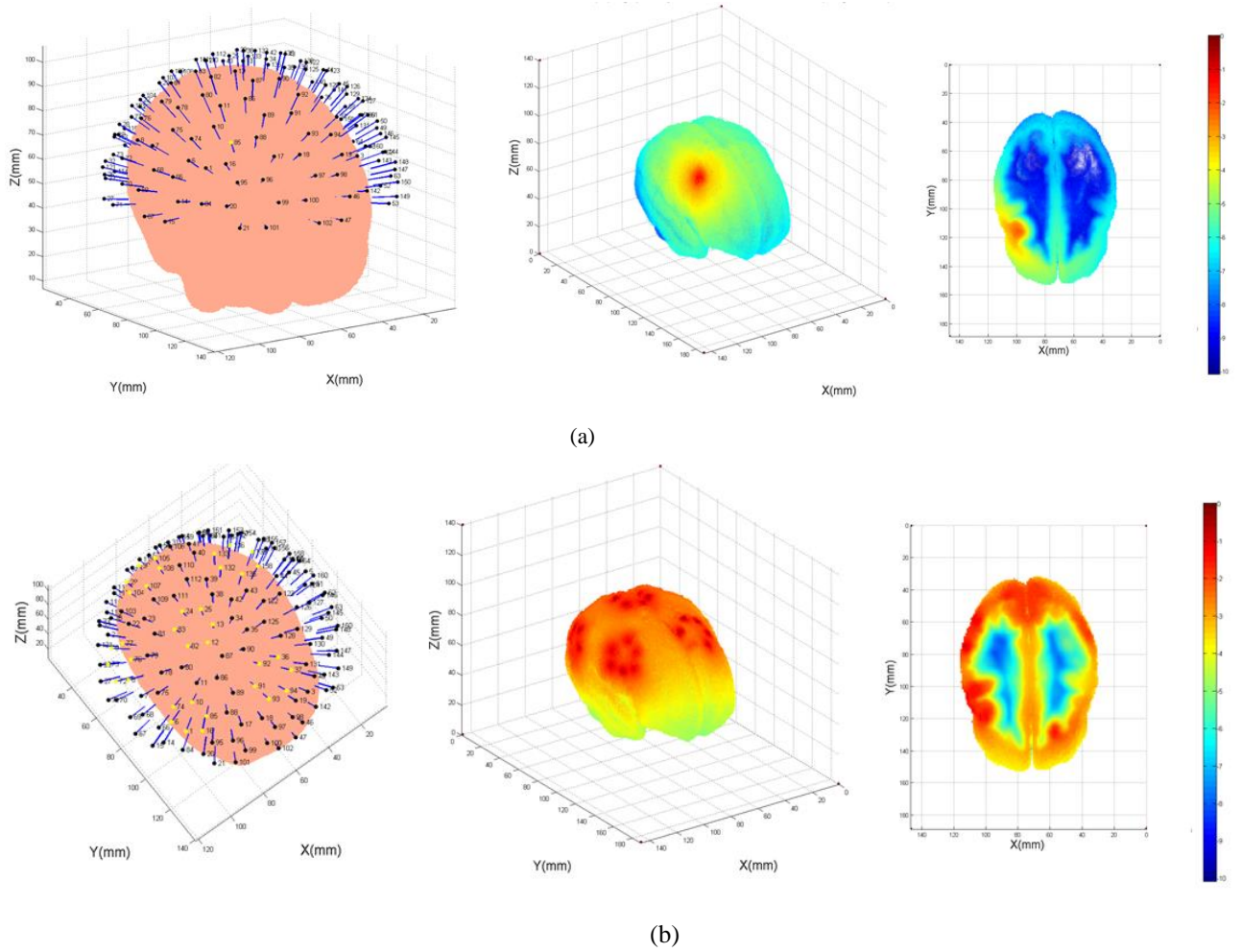


Figure 4. Fluence maps for different source configurations. (a) (left) shows the optical fibers and their IDs. Fiber no. 85 is turned on indicated with a yellow circle. (Middle) Fluence map for gray and white matter and (right) is the same fluence map but from a cross-sectional cut. (b) the same as previous but for a different set of fibers indicated with yellow circles.

3.2 Optimum answer for a special case

Here we demonstrate the result of the optimizations problem for one specific case, a uniformly distributed fluence with constant total fluence over the whole region. First, we fix F_0 such that the total fluence is 800, the corresponding fluence map is shown in Fig. 5(a). Using the genetic algorithm, we obtained the following optimal result,

$$x = [010001100101001001011100101010011 \\ 100000100111110101011010100111010$$

```

100111000101111011110011010111011
010100101101101011100100111011011
0101010100110001110111010111, 1.6];

```

This result means that the diameter of the light sources should be 1:6 mm, and 88 light sources should be turned on. Note that in this case numerical aperture was not an optimization parameter and for all optical fibers NA=0.3. Fig. 5(b) shows the obtained fluence map for this answer.

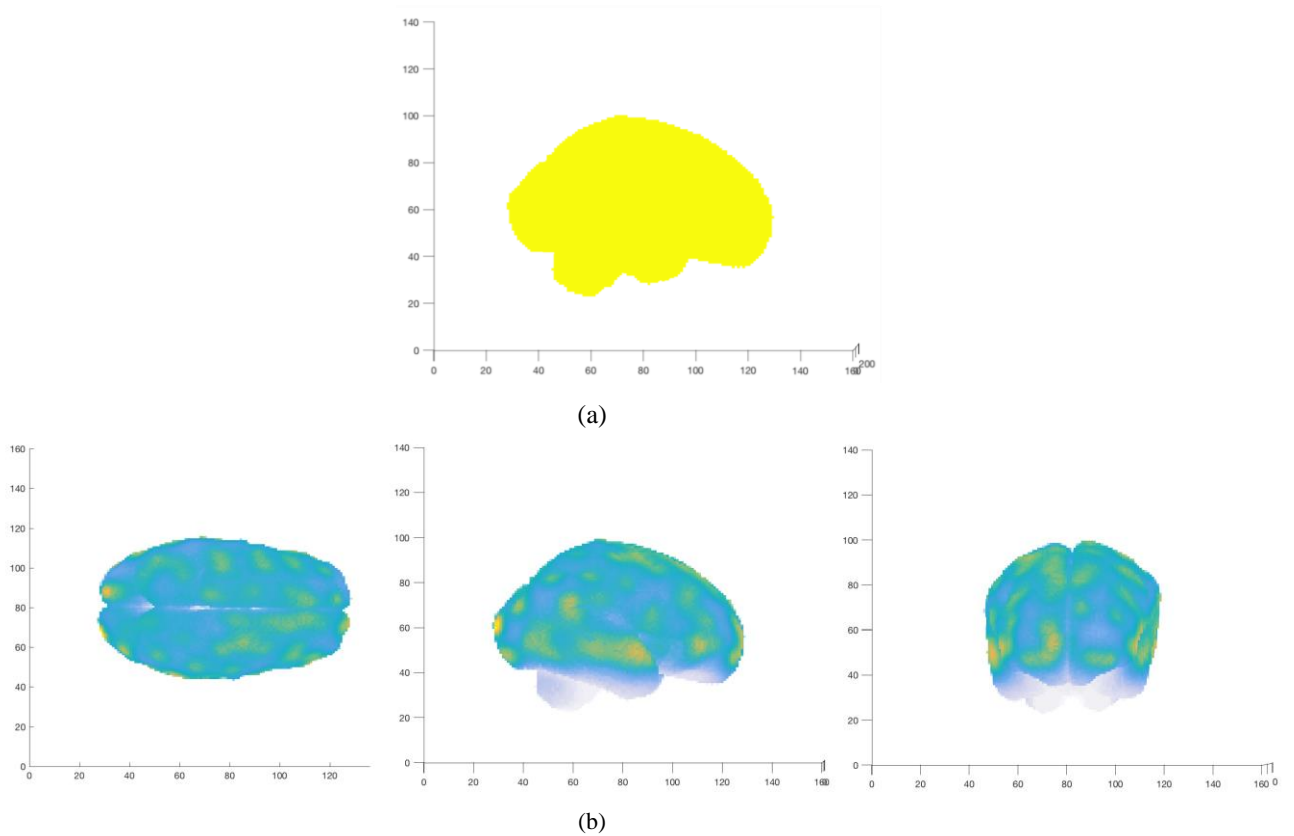


Figure 5. Optimization problem. (a) Desired (initial) fluence map, (b) the best fluence map returned from GA method which is obtainable with the available dataset.

4. CONCLUSION

Having a uniform fluence distribution inside the imaging object, makes the reconstructed photoacoustic images a more accurate representation of absorption coefficient. In this study we presented a method for achieving uniform illumination. Using Monte Carlo simulations we created a large dataset of fluence maps for 260 optical fibers for different diameters and numerical apertures. Using this dataset we tried to obtain a fluence map as close as possible to our desired fluence map which was uniform. Although, the entirely uniform distribution could not be obtained, this was the closest answer with the available dataset. At this point the numerical aperture was not an optimization parameter and it was fixed at NA=0.3. In the other hand, while different diameters were

used for optimization, yet, all fibers had the same diameter meaning that the diameter of all fibers were changing together. In the future works we want to change the NA and diameter of each fiber individually. This could improve the answer to the optimization problem.

REFERENCES

- [1] Wang, L.V. and S. Hu, Photoacoustic tomography, "in vivo imaging from organelles to organs," *Science*, 335(6075), 1458-1462 (2012).
- [2] Hariri, A., Fatima, A., Mohammadian, N., Mahmoodkalayeh, S., Ansari, M. A., Bely, N., Avanaki, M. R. N., "Development of low-cost photoacoustic imaging systems using very low-energy pulsed laser diodes," *Journal of Biomedical Optics*, 22(7), 075001 (2017).
- [3] Hariri, A., Fatima, A., Mohammadian, N., Bely, N., Avanaki, M. R. N., "Toward low cost photoacoustic spectroscopy system for evaluation of skin health," In *SPIE Optical Engineering+ Applications*, International Society for Optics and Photonics, (2016).
- [4] Wang, L.V. and Yao, J., "A practical guide to photoacoustic tomography in the life sciences," *Nature Methods*, 13(8) (2016).
- [5] Avanaki, M. R. N., Xia, J., Wan, H., Bauer, A. Q., Culver, J. P., and Wang, L. V., "High-resolution photoacoustic resting-state functional connectivity imaging of the mouse brain," *Proceedings of the National Academy of Sciences (PNAS)*, 111, no. 1, 21-26 (2014).
- [6] Wang, X., Pang, Y., Ku, G., Stoica, G., Wang, L. H., "Three-dimensional laser-induced photoacoustic tomography of mouse brain with the skin and skull intact," *Optics letters*, 28(19), 1739-1741 (2003).
- [7] Avanaki, M.R., Xia, J., and Wang, L.V., "High resolution functional photoacoustic computed tomography of the mouse brain during electrical stimulation," in *SPIE BiOS*, International Society for Optics and Photonics (2013).
- [8] Wang, X., Xie, X., Ku, G., Wang, L. H., Stoica, G., "Noninvasive imaging of hemoglobin concentration and oxygenation in the rat brain using high-resolution photoacoustic tomography," *Journal of biomedical optics*, 11(2), 024015-024015-9 (2006).
- [9] Wang, X., Chamberland, D. L., Xi, G., "Noninvasive reflection mode photoacoustic imaging through infant skull toward imaging of neonatal brains," *Journal of Neuroscience Methods*, 168(2), 412-421 (2008).
- [10] Mohammadi-Nejad, A.R., Mahmoudzadeh, M., Hassanpour, M.S., Wallois, F., Muzik, O., Papadelis, C., Hansen, A., Soltanian-Zadeh, H., Gelovani, J. and Nasiriavanaki, M., "Neonatal brain resting-state functional connectivity imaging modalities," *Photoacoustics* (2018).
- [11] Meimani, N., Abani, N., Gelovani, J., and Avanaki, M. R. N., "A numerical analysis of a semi-dry coupling configuration in photoacoustic computed tomography for infant brain imaging," *Photoacoustics*, 7, 27-35, 2017.
- [12] Wang, L., Zhang, C. and Wang, L. V. "Grüneisen relaxation photoacoustic microscopy," *Phys. Rev. Letters* 113, 174301 (2014).
- [13] Mahmoodkalayeh, S., Jooya, H. Z., Hariri, A., Zhou, Y., Xu, Q., Ansari, M. A., and Avanaki, M. R. N., "Low temperature-mediated enhancement of photoacoustic imaging depth," *arXiv preprint arXiv:1802.07114* (2018).
- [14] Mozaffarzadeh, M., Mahloojifar, A., Orooji, M., Adabi, S. and Nasiriavanaki, M., "Double-Stage Delay Multiply and Sum Beamforming Algorithm: Application to Linear-Array Photoacoustic Imaging," *IEEE Transactions on Biomedical Engineering*, 65(1), 31-42 (2018).
- [15] Wang, Z., Ha, S. and Kim, K., "A new design of light illumination scheme for deep tissue photoacoustic imaging," *Opt. Express*. 20, 22649-22659 (2012).

- [16] Brigadoi, S., Alijbar, P., Kuklisova-Murgasova, M., Arridge, S. R., Cooper, R. J., "A 4D neonatal head model for diffuse optical imaging of pre-term to term infants," *NeuroImage* 100, 385-394 (2014).
- [17] Brigadoi, S. and Cooper, R. J., "How short is short? Optimum source–detector distance for short-separation channels in functional near-infrared spectroscopy," *Neurophotonics*, 2(2), 025005 (2015).
- [18] Fang, Q. and Boas, D. A., "Monte Carlo Simulation of Photon Migration in 3D Turbid Media Accelerated by Graphics Processing Units," *Optics Express*, 17(22), 20178-20190 (2009).
- [19] Mitchell, Melanie. "An introduction to genetic algorithms". MIT press, (1998).
- [20] Whitley, Darrell. "A genetic algorithm tutorial," *Statistics and computing* 4.2, 65-85 (1994).
- [21] Akbari, R. and Ziarati, K., "A multilevel evolutionary algorithm for optimizing numerical functions," *International Journal of Industrial Engineering Computations* 2(2), 419-430 (2011).